TECHNICAL NOTE

Effects of ageing on the hydraulics of water wells and the influence of non-Darcy flow

Georg J. Houben[1] · Julia Wachenhausen[1] · Carlos R. Guevara Morel[1]

Abstract

Well ageing is mostly caused by mechanical and biogeochemical clogging processes, which affect the gravel pack, screen slots and casing. Clogging deposits increase head losses due to a constriction of the hydraulically effective area. For this study, clogging is mimicked by systematically reducing the gravel pack porosity, the screen open area and the nominal inner casing diameter. Groundwater flow velocity strongly increases close to the well, inducing inertial and turbulent flow components. Therefore, gravel pack head losses were calculated using the Forchheimer-Engelund equation, in conjunction with the Kozeny-Carman equation, which relates gravel pack porosity and hydraulic conductivity. Screen losses were assessed using the Orifice equation and turbulent casing losses with the Darcy-Weisbach equation. For the settings chosen here, a dramatic increase of head losses occurs when the clogging has reduced the effective porosity in the gravel pack by ~65%, the open area of the screen by ≥98%, and the casing diameter by ~50%. Since the latter two conditions are rarely reached in actual wells, the clogging of the gravel pack is the decisive parameter that controls well ageing. Regular monitoring of the well yield is therefore needed, since processes in the gravel pack are difficult to track directly. Unlike the deposits on the casing and in the screen slots, obstructions in the gravel pack are much more difficult to remove.

Keywords Groundwater hydraulics · Well enhancement · Ageing · Clogging · Non-Darcy flow

Introduction

Knowledge about the hydraulics of water wells is important for the evaluation of hydraulic tests and the design of energy-efficient wells. The topic has been addressed in a multitude of publications, reviews and textbooks (e.g. Driscoll 1986; Roscoe Moss Company 1990; Barker and Herbert 1992a, b; Vukovic and Soro 1992; Parsons 1994; Houben 2015a, b). However, most studies consider the well in its initial, pristine state, immediately after drilling and development, when in reality, operating wells suffer from ageing, which manifests itself as a decrease of well yield or, in other words, an increase of drawdown over time. This is mostly caused by the obstruction of flow paths through the gradual deposition of solid

material. Processes that can induce such a clogging include the deposition of mineral phases (e.g. iron and manganese oxides, calcite), the growth of biofilms and the invasion of particles (Houben 2003; Houben and Treskatis 2007). Deposits can cause a loss of porosity in the gravel pack, a reduction of the open area of the screen and a decrease of the effective (inner) casing diameter.

It is thus imperative and the objective of this study to assess the impact of permeability-impairment by well ageing on the hydraulics of the well, but also to which degree non-Darcy flow processes are involved. In the radial flow field around a well, velocities have to increase sharply close to its axis, potentially inducing deviations from the linear laminar flow regime. Clogging will further decrease the area available for flow, thereby increasing velocity and non-Darcy flow even further. The admixture of clogging particles and minerals to an initially homogeneous gravel pack will have the same effect (van Lopik et al. 2017). Therefore, a quantitative relationship between the open area, here the porosity of the gravel pack, the open screen area and the effective casing diameter, respectively, and the linear laminar, non-linear laminar and turbulent head losses is established.

✉ Georg J. Houben
  georg.houben@bgr.de

[1] Federal Institute for Geosciences and Natural Resources (BGR), Stilleweg 2, 30655 Hannover, Germany

Table 1 Inertial (non-Darcy) coefficient equations for porous media

Model	β	Unit	Material/ media	Reference
$1.82 \times 10^8 k^{-5/4} n^{-3/4}$	cm^{-1}	mD	Porous media	Janicek and Katz (1944)
$0.005 k^{-1/2} n^{-11/2}$	cm^{-1}	cm^2	Sandstone, unconsolidated	Geertsma (1974)
$0.5 K^{1/2}$	–	cm s^{-1}	Unconsolidated sediments	Cox, as cited in Barker and Herbert (1992b)
$2.94 \times 10^7 \tau k^{-1} n^{-1}$	cm^{-1}	mD	Consolidated/unconsolidated porous media	Liu et al. (1995)
$1.07 \times 10^{12} k^{-1.88} n^{0.449}$	ft^{-1}	mD	Dry and saturated core samples	Coles and Hartman (1998)
$2.5 \times 10^5 k^{-1}$	cm^{-1}	D	Porous media	Thauvin and Mohanty (1998)
$17.2 \times 10^{10} k^{-1.76}$	ft^{-1}	mD	Unconsolidated porous media	Khaniaminjan and Goudarzi (2008)
$0.5 K^{-1/2}$	–	cm s^{-1}	Unconsolidated sediments	Modified Cox cited in Houben (2015a)

* *K* hydraulic conductivity; *k* permeability; *τ* tortuosity; *n* porosity; *mD* milliDarcy; D Darcy. 1 ft. = 0.3048 m

Non-linear and turbulent flow can also accelerate clogging processes, since turbulence leads to better mixing. This potentially increases the probability of a collision of crystallization seeds, brings reaction partners together (e.g. ferrous iron and dissolved oxygen) and enhances the nutrient supply to biofilms (Houben and Treskatis 2007). In this regard, clogging induced by non-Darcian flow could actually be a self-promoting process.

Non-Darcy flow in the nearfield of wells

Deviations from linear laminar Darcy flow can occur in regions of high flow velocities due to the appearance of inertial effects. Non-Darcy flow is therefore particularly interesting for near-well regions, where flow velocities increase drastically due to a reduction of the available hydraulic area.

Typically, the description of non-linear laminar (non-Darcy) flow is done using the Forchheimer equation (Forchheimer 1901a, b), which can be expressed as (Bear 1972):

$$\frac{dh}{dx} = \propto q + \beta q^2 = \frac{\mu}{k\rho g} q + \frac{\beta'}{g} q^2 \qquad (1)$$

where $\alpha = 1/K$ and $\beta = \beta'/g$ and the other terms are as listed:

h	head [L]
x	distance [L]
q	specific flux [L T^{-1}]
K	hydraulic conductivity [L T^{-1}]
k	permeability [L^2]
ρ	fluid density [M L^{-3}]
μ	fluid dynamic viscosity [M L^{-1} T^{-1}]
g	gravitational acceleration [L T^{-2}]
β	inertial or Forchheimer coefficient [T^2 L^{-2}]

Fig. 1 Inertial (non-Darcy) coefficients $\beta*$ as a function of porosity, calculated using the equations given in Table 1. The dashed lines represent coefficients for unconsolidated materials, the solid lines for consolidated materials
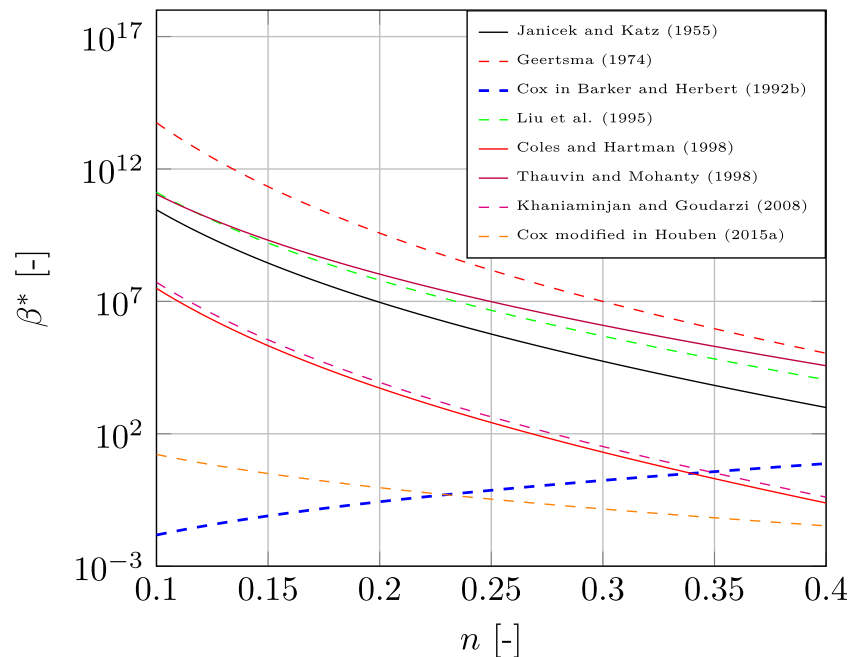
Table 2 Parameters and values used for example calculations

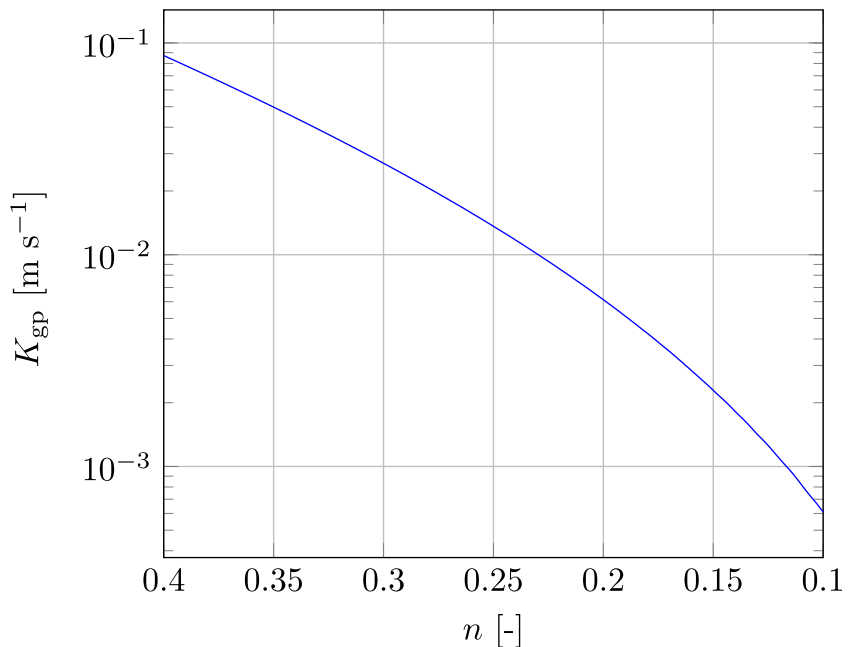| Parameter	Symbol	Value	Unit
Pump rate	Q	75 (150)	$m^3 s^{-1}$
Aquifer thickness	B	20	m
Casing diameter	d_p	300	mm
Mean grain size of gravel pack	d_{50}	3.0	mm
Porosity of gravel pack	n	0.10–0.40	–
Radius of borehole	r_b	0.225	m
Radius of screen	r_s	0.125	m
Length of screen	L_s	20	m
Slot width	W_{sl}	1.5	mm
Contraction coefficient	C_c	0.62	–
Velocity coefficient	C_v	0.98	–
Distance to pump (in casing)	L_p	20	m
Roughness of casing	κ	0.06	mm
Density of fluid	ρ	1000	$kg\ m^{-3}$
Viscosity of fluid	μ	0.001	$kg\ m^{-1}\ s^{-1}$
Acceleration of gravity	g	9.81	$m^2\ s^{-1}$
Tortuosity	τ	1.0	–

For radially symmetric steady-state non-Darcian flow in a confined aquifer towards a well, the analytical model from Engelund (1953) can be used to calculate drawdown:

$$s = \frac{Q}{2\pi KB} ln\left(\frac{r_2}{r_1}\right) + \beta^*\left(\frac{Q}{2\pi KB}\right)^2\left(\frac{1}{r_1} - \frac{1}{r_2}\right) \quad (2)$$

where $r_2 > r_1$ and:

s drawdown [L]
Q pumping rate $[L^3\ T^{-1}]$

B aquifer thickness [L]
r_2 outer radius [L]
r_1 inner radius [L]
β^* inertial or Forchheimer coefficient [−]

For the gravel pack, r_2 = drilling radius r_b, r_1 = screen radius r_s, and K = gravel pack hydraulic conductivity K_{gp}.

Depending on the form of the Forchheimer equation used, the inertial coefficient will have different units (Houben 2015a). The inertial coefficients β^* [−], β' $[L^{-1}]$ and β $[T^2 L^{-2}]$ are related as follows:

$$\beta^* = \frac{\beta}{K^2} = \frac{\beta'}{gK^2} \quad (3)$$

The inertial coefficient is usually determined through physical experiments and is influenced by the properties of the porous media (Houben 2015a; Van Lopik et al. 2017). Muljadi et al. (2016) compared various experimental formulations of β' against estimated values from non-Darcy-flow-pore-scale simulations. They found that their obtained β' are comparable with the experimental formulations. More recently, Sharma et al. (2017) made a thorough literature review of existing non-Darcy coefficient formulations, detailing the type of media for which each coefficient is used. Table 1 presents a list of selected inertial coefficient formulations used for porous media.

Figure 1 depicts the equations from Table 1 (as β^*) as a function of porosity. Corresponding permeabilities (or hydraulic conductivities) were calculated using Eq. (5), using the parameters in Table 2. There is wide range of values obtained from the different formulations; however, the Cox (1977), cited in Barker and Herbert (1992b), does not follow

Fig. 2 Gravel pack hydraulic conductivity K_{gp} [m s^{-1}] (Eq. 5) as a function of gravel pack porosity n [−] calculated using Eq. (5)

the trend of the other formulations, which all predict an increasing inertial coeffcient value with decreasing porosity. It is assumed that a minus sign is missing in the exponent of the equation by Cox (1977) in Barker and Herbert (1992b). If this sign is added, the Cox equation (called "Cox, modified" in Fig. 1) behaves similar to the other equations and makes more physical sense.

Therefore, the Forchheimer coefficient β^* is calculated here following the modified Cox equation, as already used in Houben (2015a), as:

$$\beta^* = 0.5 \left(K_{gp} \right)^{-1.25} \tag{4}$$

in which K_{gp} should have the unit of cm s^{-1}. Despite this inconsistency in units, β^* is dimensionless (Houben 2015a).

Since ageing involves a change in gravel pack porosity, the Kozeny-Carman equation (Kozeny 1953) will be used to relate porosity to hydraulic conductivity, here in the form proposed by Bear (1972) as:

$$K_{gp} = \left(\frac{n^3}{(1-n)^2} \right) \left(\frac{d_{50}^2}{180} \right) \left(\frac{\rho g}{\mu} \right) \tag{5}$$

where the following list applies:

K_{gp} hydraulic conductivity of gravel pack [L T^{-1}]
n porosity of gravel pack [−]
d_{50} mean grain size of gravel pack [L]

For the sake of simplicity, effects of well ageing on the roughness and the shape of the pores of the gravel pack, which could be addressed in an expanded form of the Kozeny-

Carman equation, will be ignored. Unlike the porosity, which shows a cubic effect on the hydraulic conductivity, both parameters have a less pronounced influence on hydraulic conductivity and do not vary over a wide range; therefore, this simplification is justified.

Head losses occurring in a screen receiving uniform flow can be obtained using the orifice equation (Barker and Herbert 1992a; Parsons 1994):

$$s_{sc} = \frac{1}{2g} \left(\frac{Q}{2\pi L_s C_v C_c A_p} \right)^2 \tag{6}$$

where

s_{sc} screen head losses [L]
C_v slot velocity coefficient (~0.98) [−]
C_c contraction coefficient (~0.66) [−]
A_p fractional open area (screen open area / screen total area) [−]

Screen ageing was mimicked by reducing only the open area. Effects on the velocity and contraction coefficients were ignored.
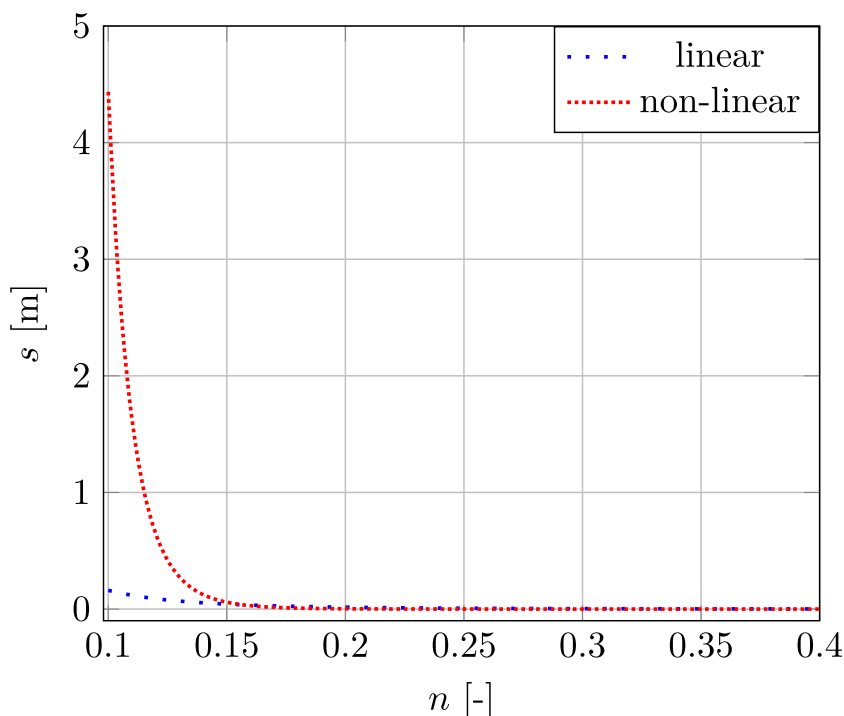
Upflow losses s_{up}, in a pipeline, e.g. a casing, were computed using the Darcy-Weisbach equation for turbulent flow (Weisbach 1845):

$$s_{up} = f_D \frac{L_p}{d_p} \frac{v^2}{2g} = f_D \frac{L_p}{d_p} \frac{(Q/A)^2}{2g} \tag{7}$$

where

L_p pipe length [L]

Fig. 3 Linear laminar and non-linear laminar gravel pack head losses, calculated using Eq. (2) as a function of the gravel pack porosity for $Q = 75$ m^3 h^{-1}

d_p (inner) pipe diameter [L]
A pipe area [L^2]
f_D Darcy friction factor [−]

The friction factor is calculated here using the Moody (1944) approximation as:

$$f_D = 0.0055 \left[1 + \left(20000 \frac{\kappa}{d_p} + \frac{10^6}{\text{Re}} \right)^{\frac{1}{3}} \right] \tag{8}$$

which is valid for Reynolds numbers Re of $4 \cdot 10^3 < \text{Re} < 1 \cdot 10^7$ and $\kappa/d_p \leq 0.01$ with κ = equivalent surface roughness [L].

Again, ageing was mimicked by reducing only the inner diameter. The influence of the roughness of the incrustations was not considered. The Reynolds number is defined here as (Bear 1972):

$$\text{Re} = \frac{\rho v_a d}{\mu} \tag{9}$$

where:

v_a actual porosity-corrected groundwater velocity [L T^{-1}]
d characteristic length [L]

For the gravel pack and the screen, the characteristic length equals the mean grain size d_{50} and the slot width W_{sl} [L], respectively. Furthermore, groundwater flow velocity is defined as:

$$v_a = \frac{Q}{2\pi r B F_{corr}} \tag{10}$$

where

r radial distance [L]
F_{corr} correction factor [−]

The F_{corr} is equal to n and A_p for the gravel pack and the screen, respectively. Table 2 shows the parameters and values used for the example calculations of this study. Calculations were conducted using the Microsoft Excel application Well Designer (Houben 2015b), using the equations listed above. Calculations assume radially symmetric horizontal flow to a fully penetrating well in a homogeneous, confined aquifer.

Results and discussion

The relationship between porosity and hydraulic conductivity of gravel pack material, according to the Kozeny-Carman equation (Eq. 5), is shown in Fig. 2. Due to their coarse granulometry, well-rounded grains and good sorting, gravel packs may have initial porosities as high as 35% and more. They undergo a decrease in hydraulic conductivity of up to three orders of magnitude when the porosity is reduced to 10%

and less, which is typical for clogging processes (Houben and Treskatis 2007).

The curve shape in Fig. 2 roughly resembles typical ageing curves of water wells, where yield is plotted as a function of time (Vukovic and Soro 1992; Houben and Treskatis 2007). Houben and Treskatis (2007) had already invoked the Kozeny-Carman equation to explain the ageing curves of actual water wells. This was, however, done qualitatively and with only linear laminar flow in mind. In reality, these ageing
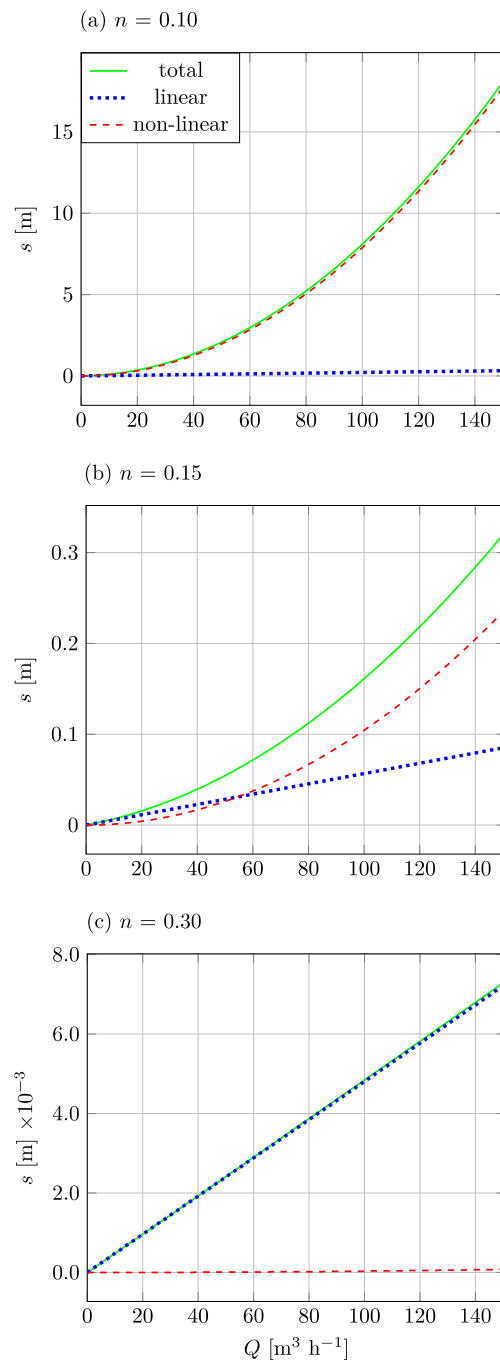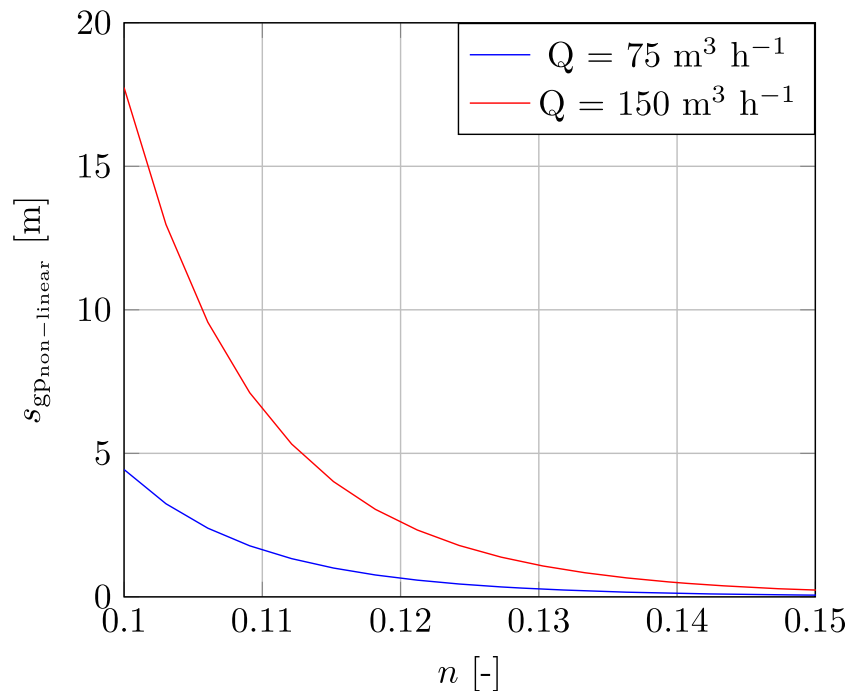

Fig. 4 Head loss s as a function of pumping rate Q for porosity n values of **a** 0.10, **b** 0.15 and **c** 0.30, calculated using Eq. (2)

Fig. 5 Gravel pack non-linear head losses as a function of gravel pack porosity n for pumping rates $Q = 75$ and 150 m^3 h^{-1}, using Eq. (2)

curves often do not show a noticeable yield decrease in the first years, that is, the curve is almost horizontal for some time, suggesting that a simple porosity–ageing relation is not a sufficient explanation for the behavior observed in the field.

Therefore, the ageing was assessed here taking non-Darcy flow into account. The shrinking porosity was used to obtain the hydraulic conductivity according to the Kozeny-Carman equation. Then, this was used to calculate the linear laminar and non-linear laminar gravel pack head losses as function of gravel pack porosity with the Forchheimer-Engelund approach. As can be seen in Fig. 3, the clogging-induced reduction of the porosity initially has a comparably small effect on

head losses. This is explained by the location of the first clogging deposits, which usually occur at the edges of the pores, playing a minor role regarding flow. However, at residual porosities of about 15%, noticeable losses start to occur, while at porosities below 12%, about a third of the initial, the non-linear losses become dominant and increase dramatically. This increase is explained mathematically by the relative importance of the non-linear laminar term in Eq. (2), which displays a square dependency between conductivity and head loss. While a change in hydraulic conductivity is related linearly to the laminar losses, a decrease by a factor of two will lead to a quadrupled head loss in the non-linear laminar term.

Fig. 6 Reynolds number Re (red) and actual flow velocity v_a (blue) in the gravel pack at a radial distance $r_b = 0.225$ m (borehole wall) as a function of the gravel pack porosity n, for pumping rates $Q = 75$ and 150 m^3 h^{-1} (Eqs. 9 and 10)
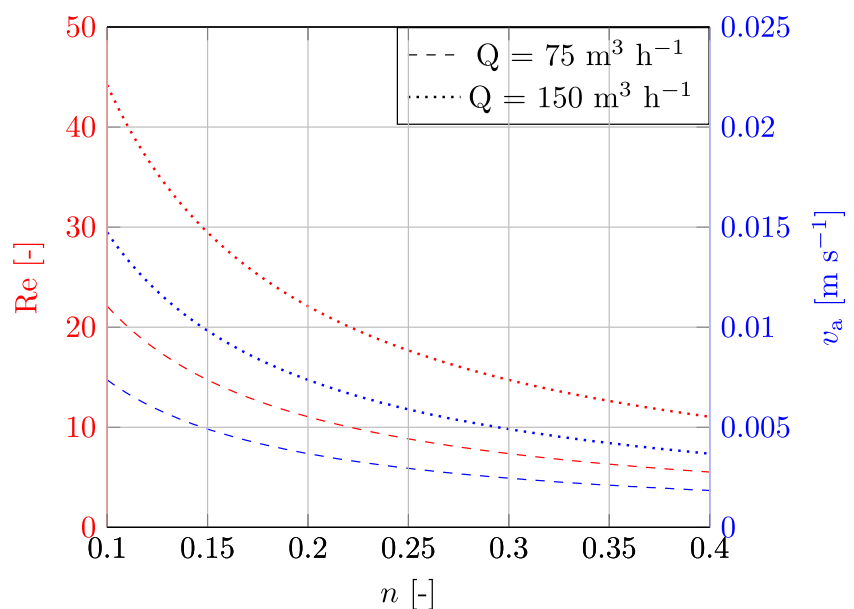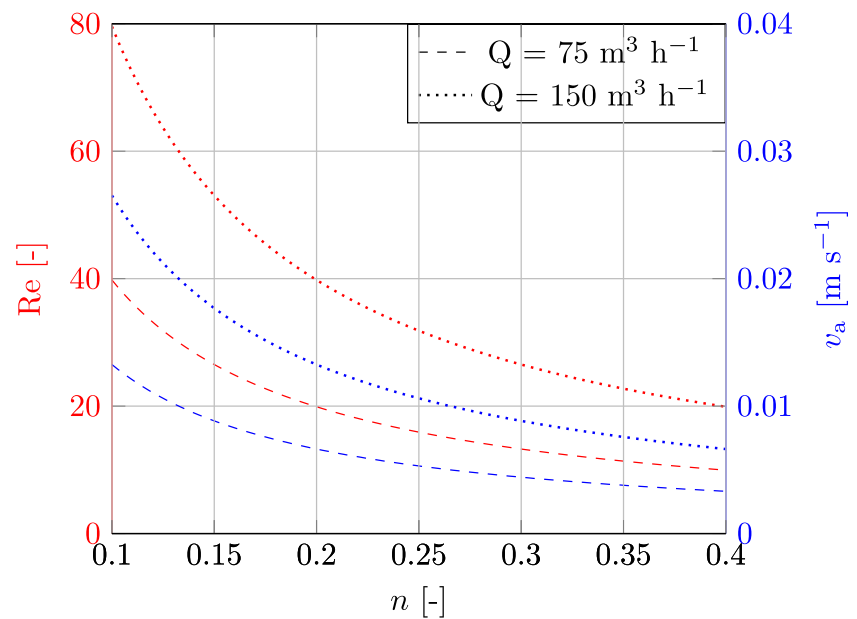
Fig. 7 Reynolds number Re (red) and actual flow velocity v_a (blue) in the gravel pack at a radial distance $r_s = 0.125$ m (screen face) as a function of the gravel pack porosity n, for pumping rates $Q = 75$ and 150 m³ h⁻¹ (Eqs. 9 and 10)

Physically, during non-linear flow, clogging materials start obstructing the main flow channels which lead to the formation of flow vortices (eddies), consequently reducing the effective area available for flow and thus hydraulic conductivity (Chauveteau and Thirriot 1967; Chaudary et al. 2011; Muljadi et al. 2016). If only Darcian flow, that is laminar losses, were considered, this dramatic development would go unnoticed. The curve shape in Fig. 3 resembles actual ageing curves of wells much more closely than that shown in Fig. 2.

Figure 4 shows the head losses as a function of the pumping rate for porosity values n of 0.10, 0.15 and 0.30.

Above even relatively low pumping rates ($Q \approx 30$ m³ h⁻¹), a low porosity will induce strong non-linear head losses. Figure 5 depicts only the non-linear head losses in the gravel pack for two pumping rates. Again, at porosities <11%, the non-linear head losses increase by a factor of about three as the pumping rate is doubled, which, again, emphasizes the drastic head loss increase as porosity reduces and velocities increase in the gravel pack.

Figures 6 and 7 show the Reynolds numbers Re and the actual flow velocities v_a in the gravel pack at the borehole wall (Fig. 6, entering the gravel pack, $r_b = 0.225$ m) and at the

Fig. 8 Screen head losses calculated using the orifice equation (Eq. 6) as a function of the screen open area A_p, for pumping rates $Q = 75$ and 150 m³ h⁻¹

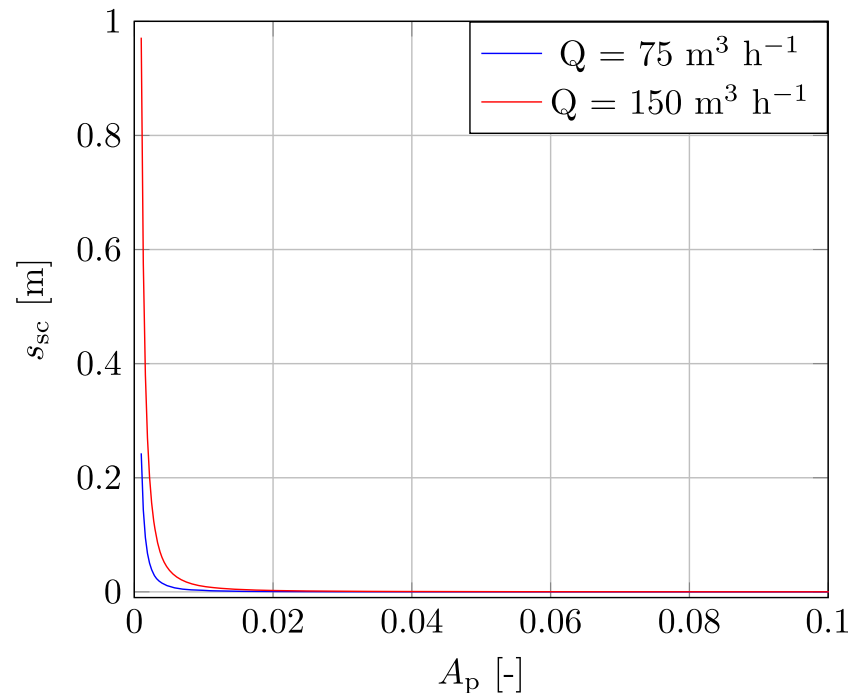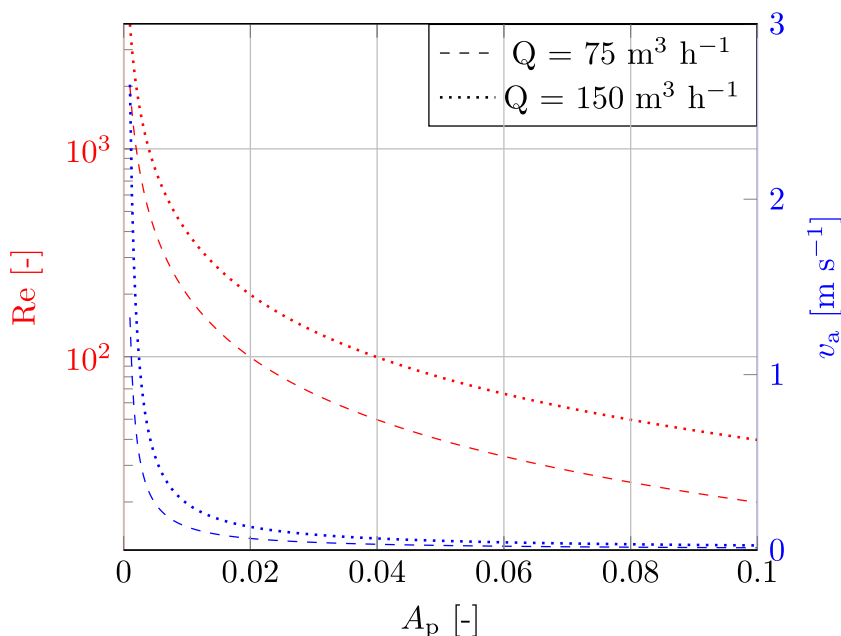screen face (Fig. 7, $r_s = 0.125$ m) as a function of gravel pack porosity. The boundary between linear laminar and non-linear laminar flow is not well defined, but is often assumed to be in the range of Re = 1 to 10 (Bear 1972). For the pumping rates selected here, predominantly non-linear laminar flow is observed in the gravel pack and the Reynolds numbers accordingly indicate non-laminar flow conditions.

The flow velocity also has to increase with increasing porosity reduction. Well designers often use a "critical" entrance velocity of 0.03 m s^{-1} at the screen face (Houben 2015a),

which should not be exceeded to avoid losses and enhanced ageing. There is, however, considerable debate about the validity of this number and some planners allow much higher velocities (see discussion in Houben 2015a). In the cases considered here, entrance velocities get close to this value for low porosities and high pumping rates (Fig. 7).

Permeability-impairing deposits are not necessarily restricted to the gravel pack, but may also occur in the adjacent aquifer (Houben and Weihe 2010). Particle accumulation at the borehole wall may induce the formation of a wellbore skin

Fig. 10 Casing upflow losses calculated using the Darcy-Weisbach (Eq. 7) as a function of the effective (inner) pipe diameter d_e, for pumping rates $Q = 75$ and 150 m^3 h^{-1}. Please note that the effective diameter d_e is given here as a relative value with $d_e = d_o/d_p$ (d_o = open diameter, d_p = initial unclogged diameter). Casing length 20 m
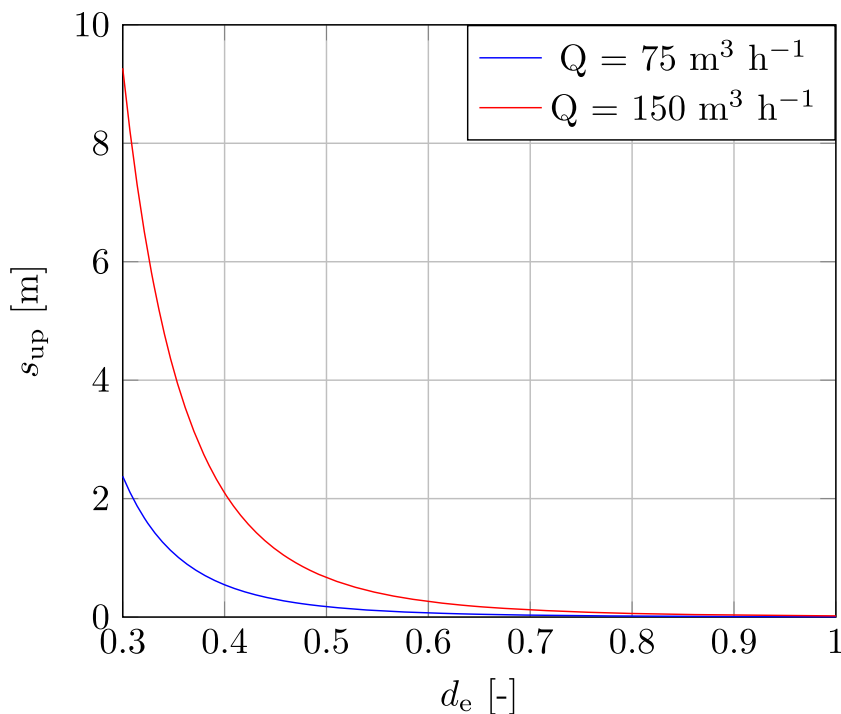
layer, that also causes increased head losses (Houben et al. 2016); both processes, however, are not addressed here. The porosity of the gravel pack can also be reduced by settling (compaction), caused by mechanical agitation, e.g. during well development, switching on and off the pump, maintenance and inspection (tripping in and out of pump, equipment and probes), mechanical rehabilitations and, finally, earth quakes (Houben and Treskatis 2007).

Figure 8 shows the screen losses (Eq. 6) as a function of the open area of the screen. Only at extremely high degrees of clogging, when 98% or more of the slot area is blocked, will losses rise dramatically. This confirms calculations by Huisman (1972), who came to similar conclusions. Only at his ultimate stage will screen losses reach a detectable level. Compared to the losses obtained for a clogged gravel pack (residual porosity 10%, Figs. 2 and 3), the losses in an almost completely blocked screen are about an order of magnitude smaller.

The Reynolds number Re and the actual flow velocity v_a entering the screen ($r_s = 0.125$ m) are shown in Fig. 9. As expected, a transition from non-linear laminar flow to turbulent flow occurs at higher flow rates. It is evident that a sudden increase in Reynolds number occurs after ~98% of the screen slots have been clogged and flow becomes fully turbulent.

The upflow losses caused by a 20 m casing are shown in Fig. 10 as a function of the effective (inner) pipe diameter (effects of roughness not considered). They are not significant when the pipe diameter is reduced by 30% or less. A considerable increase in the upflow head losses occurs when the pipe has only 50% of its initial effective diameter. From this point on, losses start to grow exponentially and reach values similar to those caused by the clogging gravel pack. It should be noted that the relative contribution of the upflow losses can be higher in deeper wells with longer casing and riser pipes.

So far, the ageing of the three compartments gravel pack, screen and casing was treated individually here. In reality, all parts of the well will be affected by clogging processes more or less at the same time. The ageing curve of the well will thus reflect the sum of all processes. Camera inspections give good insights into the degree of and, to some extent, the spatial distribution of clogging. They often reveal casing interiors covered by incrustations or biofilms of up to several centimeters thickness (e.g. Houben and Treskatis 2007). A reduction of the effective diameter by 50% and more is, however, rarely seen and commonly operators would take measures before it comes to this. Camera inspections also often show serious clogging of screen slots, but a closure of 98% and more is rarely seen and would, again, surely motivate countermeasures. It is thus concluded that large parts of the head losses from well ageing observed in the field must come from gravel pack clogging. This, however, is difficult to observe and track. Camera inspections will only allow a view of a few grains close to the screen slots, which might not be representative. Due to the rather sudden increase of losses at low porosities, the best choice is to constantly track the well yield, measured as a ratio of pumping rate and drawdown (Houben and Treskatis 2007).

Summary and conclusions

Well ageing can be considered the sum of the head losses caused by the clogging of casing, screen and gravel pack (and potentially other compartments). Head losses in the gravel pack are induced by a reduction of porosity through mechanical compaction and the deposition of minerals, biomass and particles. After around two thirds of the initial pore space of the gravel pack have been blocked, a dramatic increase of non-linear laminar head losses occurs. Purely Darcian models are thus not adequate to investigate the hydraulic effects of well ageing. Losses in the screen slots become noticeable only very late in the clogging process, when almost all (> 98%) of the open screen area has been blocked. At this point, a drastic increase in the flow turbulence occurs. Upflow losses in the casing start to be relevant when the effective (inner) pipe diameter has decreased by approximately 50%. Further reduction of the pipe diameter will exponentially accelerate upflow losses. Such heavy incrustations of casing and screen slots are, however, rather uncommon and easily reversed. Therefore, gravel pack clogging probably plays the most important role in well ageing. Unfortunately, it is much more difficult to identify and to remove.

Even simple well rehabilitation techniques such as brushing are able to clean the slots and the casing interior. A complete restoration of the porosity of the gravel pack to its initial state, on the other hand, is difficult and costly, even with advanced rehabilitation methods. Pushing back the ageing curve to its initial stage is thus seldom possible. Ageing often accelerates after the rehabilitation and the ageing curve will go down faster, as it now starts from an advanced stage on the curve (Houben and Treskatis 2007).

The ageing processes of the three compartments studied here share the peculiar behavior that losses tend to increase rather suddenly and dramatically after some point. It is therefore of utmost importance to track the yield curve of a well continuously (or at regular intervals) over its life cycle, which allows for reaction before the "point of no return" is passed. Commonly, a maximum loss of 10–20% of the initial yield is used as an alarm to induce rehabilitation (Houben and Treskatis 2007).

References

Barker J, Herbert R (1992a) Hydraulic tests on well screens. Appl Hydrogeol 0:7–19

Barker J, Herbert R (1992b) A simple theory for estimating well losses: with application to test wells in Bangladesh. Appl Hydrogeol 0:20–31

Bear J (1972) Dynamics of fluids in porous media. Dove, New York

Chaudary K, Bayani Cardenas M, Deng W, Bennett PC (2011) The role of eddies inside pores in the transition from Darcy to Forchheimer flows. Geophys Res Lett 38(24):L24405

Chauveteau G, Thirriot C (1967) Régimes d'écoulement en milieu poreux et limite de la loi de Darcy [Regimes of flow in porous media and the limitations of the Darcy law]. La Houille Blanche 1(22):1–8

Coles M, Hartman K (1998) Non-Darcy measurements in dry core and the effect of immobile liquids. SPE 39977:193–202

Driscoll FG (1986) Groundwater and wells, 2nd edn. Johnson, St. Paul, MN

Engelund F (1953) On the laminar and turbulent flow of groundwater through homogeneous sands. Technical report, Akademiet for de Tekniske Videnskaber, Copenhagen

Forchheimer P (1901a) Wasserbewegung durch Boden [Movement of water through soil]. Z Ver Dtsch Ing 45:1736–1741

Forchheimer P (1901b) Wasserbewegung durch Boden [Movement of water through soil]. Z Ver Dtsch Ing 50:1781–1788

Geertsma J (1974) Estimating the coefficient of inertial resistance in fluid flow through porous media. Soc Petrol Eng J 14(5):445–450

Houben G (2003) Iron oxide incrustations in wells, part 1: genesis, mineralogy and geochemistry. Appl Geochem 18(6):927–939

Houben G (2015a) Review: Hydraulic of water wells—flow laws and influence of geometry. Hydrogeol J 23:1633–1657

Houben G (2015b) Review: Hydraulic of water wells—head losses of individual components. Hydrogeol J 23:1659–1675

Houben G, Treskatis C (2007) Water well rehabilitation and reconstruction. McGraw Hill, New York

Houben G, Weihe U (2010) Spatial distribution of incrustations around a water well after 38 years of use. Ground Water 48(5):53–58

Houben G, Halisch M, Kaufhold S, Weidner C, Sander J, Reich M (2016) Analysis of wellbore skin sample-typology, composition, and hydraulic properties. Groundwater 54(5):634–645

Huisman L (1972) Groundwater recovery. Macmillan, Basingstoke

Janicek J, Katz D (1944) Applications of unsteady state gas flow calculations. Technical report, Proc. U. of Michigan Research Conference, Univ. of Michigan, Ann Arbor, MI

Khaniaminjan A, Goudarzi A (2008) Non-Darcy fluid flow through porous media. SPE 114019:1–19

Kozeny J (1953) Hydraulik: Ihre Grundlagen und Praktische Anwendung [Hydraulics: fundamentals and practical application]. Springer, Vienna

Liu X, Civan F, Evans R (1995) Correlation of the non-Darcy flow coefficient. J Can Petrol Technol 34

Moody L (1944) Friction factors for pipe flow. Trans Am Soc Mech Eng 66(8):671–684

Muljadi B, Blunt M, Raeini A, Bijeljic B (2016) The impact of porous media heterogeneity on non-Darcy flow behaviour from pore-scale simulations. Adv Water Resour 95:329–340

Parsons S (1994) A re-evaluation of well design procedures. Q J Eng Geol 27:S31–S40

Roscoe Moss Co. (1990) Handbook of ground water development. Wiley, New York

Sharma V, Sircar A, Mohammad N, Sannistha P (2017) A treatise on non-Darcy flow correlations in porous media. J Pet Envirom Biotechnol 8(5)

Thauvin F, Mohanty K (1998) Network modeling of non-Darcy flow through porous media. Transp Porous Med 31:19–37

Van Lopik JH, Snoeijers R, van Dooren TCGW, Raoof A, Schotting RJ (2017) The effect of grain size distribution on nonlinear flow behavior in sandy porous media. Transp Porous Med 120(1):37–66

Vukovic M, Soro A (1992) Hydraulics of water wells: theory and application. Water Resources, Littleton, CO

Weisbach J (1845) Lehrbuch der Ingenieur- und Maschinen-Mechanik [Textbook of engineering and machine mechanics]. Friedrich Vieweg, Braunschweig, Germany